SAND2022-3658C

Impact of Modeling Assumptions on Traveling Wave Protective Relays in Hardware in the Loop

Javier Hernández-Alvídrez, *Member, IEEE*, Miguel Jiménez-Aparicio, *Member, IEEE*, and Matthew J. Reno, *Senior Member, IEEE*

Electric Power Systems Research
Sandia National Laboratories
Albuquerque, NM
{jherna4, mjimene, mjreno}@sandia.gov

***Abstract*— As the legacy distance protection schemes are starting to transition from impedance-based to traveling wave (TW) time-based, it is important to perform diligent simulations prior to commissioning the TW relay. Since Control-Hardware-In-the-Loop (CHIL) simulations have recently become a common practice for power system research, this work aims to illustrate some limitations in the integration of commercially available TW relays in CHIL for transmission-level simulations. The interconnection of Frequency-Dependent (FD) with PI-modeled transmission lines, which is a common practice in CHIL, may lead to sharp reflections that ease the relaying task. However, modeling contiguous lines as FD, or the presence of certain shunt loads, may cover certain TW reflections. As a consequence, the fault location algorithm in the relay may lead to a wrong calculation. In this paper, a qualitative comparison of the performance of commercially available TW relay is carried out to show how the system modeling in CHIL may affect the fault location accuracy.**

***Index Terms*—Control-Hardware-In-the-Loop, Traveling Waves, Protective Relays, EMT simulation.**

I. INTRODUCTION

Under the paradigm of distributed generation, more renewable energy resources are gradually being incorporated into transmission and distribution power systems. Such incorporation exhibit a twofold purpose: supplying the high-energy demands of modern societies and addressing the legitimate concerns of global climate warming by lowering the contributions of carbon emissions. This fact is behind the proliferation of studies around reliability, stability, and protection that exhibit a high penetration of distributed energy resources (DER).

From a power system protection perspective, traditional distance protection is no longer suitable for detecting the fault location with a high degree of accuracy [1]. This method is based on the monitoring of voltage and current and the calculation of the equivalent phasor impedance. A fault in the system modifies the value of both magnitudes, leading to a change in impedance. Estimating the line impedance leads to a fault location. However, bi-directional power flows and the fact that inverter-based resources are not voltage sources, hinder the detection of the involved lines. This reason has rocketed the design of new algorithms based on time-domain principles. In particular, this paper discusses the emerging protection schemes that are based on Traveling Waves (TWs) detection and analysis as a consequence of a fault occurrence.

Simulation studies rely on different software packages, such as PSCAD, ATP, or Simulink. The fact that the TWs are wide-band waves, incorporating frequency components that range from just a few Hz to several MHz, implies that the software packages need to correctly model the element's response to such heterogeneous waves. The aforementioned packages include frequency-dependent (FD) models for power lines that are suitable for transient studies.

Some TW-based relays are already commercially available for the transmission level and have incorporated single and double ended fault location schemes [1]. For the purposes of this paper, a relay with these features was the one employed for the CHIL tests. All of such protection functions depend on the correct identification of the first arrival of TWs and their successive reflections. It is worth noting that the TWs are detected using a differentiator smoothing filter [2], whose frequency response can be ovserved on [3].

The information contained in the TWs can be processed in many other different ways [4]. Other proposed fault location approaches use complex signal processing techniques, such as the Wavelet Transforms (WTs) [5]-[6], Mathematical Morphology [7], or Dynamic Mode Decomposition [8] to extract valuable information. In particular, WTs perform a time-frequency decomposition, which is specially aligned with the observations on the propagations of the TW (these waves suffer from attenuation and distortion as they propagate through the system) [9]. In addition, reconstructing just the levels that are associated with the highest-frequency components provides an alternative method of filtering out the TWs.

In the first place, this paper aims to pinpoint the differences between using or not the FD line models in the three software packages. Secondly, these generated waveforms are fed into a state-of-the-art TW protection relay for the transmission level using Control-Hardware-In-the-Loop (CHIL). The relay results showed that, under certain simulation conditions, it is not able to return an accurate fault location. Finally, this work tries to shed some light on the reasons for such failures on fault location.

II. Theoretical Background

The use of simulation models that support capturing the dynamics of traveling waves (TWs) was first introduced in the early 1960s, with the Electromagnetic Transient Program (EMTP), which later set the computational numerical methods foundations for simulators like ATP, PSCAD, and Simulink. Such simulation platforms rely on the numerical solution of the current and voltage traveling waves along transmission lines, given by:

$$\frac{\partial^2 V}{\partial x^2} = LC\frac{\partial^2 V}{\partial t^2} \quad (1)$$

$$\frac{\partial^2 I}{\partial x^2} = LC\frac{\partial^2 I}{\partial t^2} \quad (2)$$

Where L and C represent the inductance per meter and the capacitance per meter of the transmission line, respectively. Derivations of the solutions of (1) and (2) are given by the classical D'Alembert formulas:

$$I(x,t) = f_1(x - vt) + f_2(x + vt) \quad (3)$$

$$V(x,t) = Z_0 f_1(x - vt) - Z_0 f_2(x + vt) \quad (4)$$

Where v is the traveling wave speed, and Z_0 is the characteristic impedance of the transmission line. Their respective values are given by:

$$v = \frac{1}{\sqrt{LC}} \quad (5)$$

$$Z_0 = \sqrt{\frac{L}{C}} \quad (6)$$

From (3) and (4), the ratio of the voltage and current waves traveling in the positive direction is the characteristic impedance. The same ratio is maintained for the voltage and current waves traveling in the negative direction but with reversed polarity. For a thorough explanation of the derivation of (1) and (2) and their respective analytical and numerical solutions, the reader is encouraged to consult references [10] and [11].

A. Traveling Waves reflections and refractions

When a traveling wave encounters an impedance discontinuity, it experiences a change in amplitude according to the boundary conditions imposed by the discontinuity, and this is followed by the initiation of a reflected and refracted traveling wave, as depicted in Figure 1. From this figure, the sub-indexes 1, 2, and 3 relate to the incident, reflected, and refracted waves, respectively. By the principle of energy conservation, both voltage and current traveling waves must be continuous at the point of the impedance discontinuity, as marked by P_1 and P_2 in Figure 1. Under this principle, the reflected and refracted traveling waves can be expressed as a function of the incident wave [10], as follows:

$$V_2 = aV_1 \quad (7)$$

$$V_3 = bV_1 \quad (8)$$

$$I_2 = \frac{-aV_1}{Z_A} \quad (9)$$

$$I_3 = \frac{bV_1}{Z_B} \quad (10)$$

Where a and b are the reflection and refraction coefficients, respectively, and are expressed by:

$$a = \frac{Z_B - Z_A}{Z_B + Z_A} \quad (11)$$

$$b = \frac{2Z_B}{Z_B + Z_A} \quad (12)$$

Equations (11) and (12) play an important role when analyzing simulation or field data using the classical lattice diagrams, which show the traveling wave reflections in a space-time fashion [1],[10].

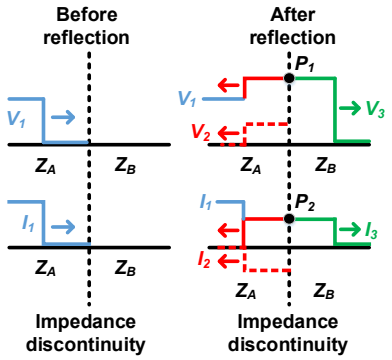

Figure 1. Traveling waves running into an impedance discontinuity.

III. Simulation System

In order to test the traveling wave dynamics under fault scenarios, the power system depicted in Figure 2 was simulated using three different electromagnetic software packages: Simulink, ATP, and PSCAD. The parameters of the different circuit elements used in the simulation model are listed in Table I. The fault analyses were performed in the transmission line labeled TL 3 in Figure 2, which for the fault modeling purposes was split into two frequency-dependent (FD) transmission line models whose total lengths add up to the 20 km of TL 3. Such FD models include the numerical solution of the partial differential equations that include the corresponding distributed parameters of the trsnamission line. This feature permits the observation of the dynamics involving the traveling waves during faults [12]. On the other hand, PI transmission line models do not include such numerical solution.

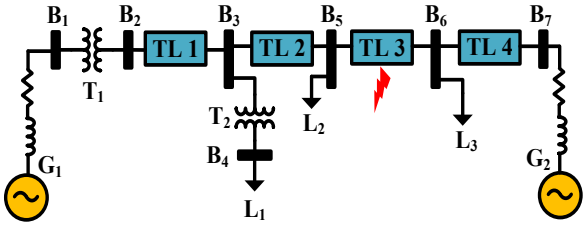

Figure 2. Diagram of the power system used for simulations.

TABLE I. SIMULATION MODEL'S PARAMETERS

Generators' Parameters			
Label	**Voltage**	**Source resistance**	**Source inductance**
G_1	161 kV	6 Ω	50 mH
G_2	138 kV	6 Ω	50 mH

Transformers' Parameters				
Label	**Configuration**	**Rating**	**Cooper Losses**	**Leakage inductance**
T_1	Yg-Yg	55 MVA	0.0008 p.u.	0.015 p.u.
T_2	Yg-Delta	10 MVA	0.0008 p.u.	0.015 p.u.

Loads' Values		
Label	**Real Power**	**Reactive Power**
L_1	4 MW	1 MVar
L_2	2 MW	0 MVar
L_3	2 MW	0 MVar

Transmission Lines' Parameters		
Label	**Length**	**Type**
TL 1	0.8 km	Frequency Dependent
TL 2	20 km	Frequency Dependent or PI
TL 3	20 km	Frequency Dependent
T L4	5.6 km	PI

The simulated single-line to ground fault over phase *a* - with a fault impedance Zf = 0.01 Ω - was applied at 8 km away to the right of bus B_5, as depicted in Figure 4. In addition, bus B_5 was selected as the bus to monitor the traveling waves of the voltages and currents used to protect TL 3 under a single-ended traveling wave protection scheme. In order to verify if a commercially available TW relay was able to detect the fault distance accurately, four simulation cases were performed.

Since a single-ended protection approach was used, the reliability of the detection of faults at bus B_5 depends upon the impedance boundary conditions at buses that create a noticeable reflection of the incident wave originated by the fault. The aforementioned simulation cases relied on changing the impedance discontinuity at bus B_5 by either: changing the value of the load impedance L_2, or changing the simulation model of transmission line TL 2.

Each simulation case was carried out using three different simulation software packages capable of handling the dynamics of traveling waves. For the Simulink simulations, a CHIL setup was used, where the voltages and currents measured at bus B_5 were directly fed into the inputs of a commercially available TW relay, as shown in Figure 3. A setup like this requires the TW relay manufacturer to customize the internal hardware and provide the required low voltage inputs suitable to receive analog signals from a real-time simulator. For this CHIL setup, the model in Figure 2 was created in Simulink and then loaded into an FPGA-based real-time simulator (OP4520 from Opal-RT Technologies) capable of handling the very stringent time resolution –less than 1 µs- required to capture the traveling waves [13]. For this CHIL Simulink simulation the time step was set to 800 ns.

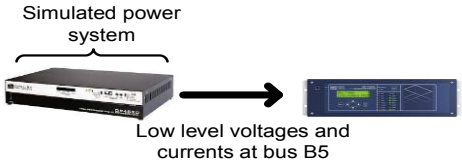

Figure 3. CHIL setup.

The simulations in ATP and PSCAD were performed offline capturing the voltage and current signals measured in bus B5. Then, these signals were converted into the proper COMTRADE format and loaded into the TW relay for its use with the event playback feature of the relay, which allows the testing and analysis of sets of signals originated from simulation studies [14]. For ATP and PSCAD, the simulation time step was set to 1 µs. Either at the end of each CHIL Simulink simulation or at the end of each event playback test, the stored traveling wave data was extracted from the relay –via COMTRADE files- for comparison with the actual current waveforms that triggered and generated such traveling waves. The results of the simulation cases are analyzed in the next section.

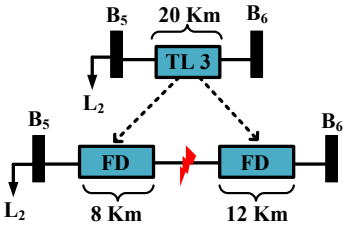

Figure 4. Detailed modeling of TL3 for simulation purposes.

IV. SIMULATION RESULTS

A. Simulation Case 1

For this case, TL 2 was modeled using a PI model and L_2 was maintained at 2 MW. The rest of the system values were the same as the ones listed in Table I.

A magnified portion of the faulted current trace right after fault inception and the corresponding TW extracted by the relay are shown in Figure 5. For all the cases, the inception time was set at t_0 = 0.11 s. The TW's first and second arrival times are given by t_1 and t_2, respectively. Based upon the single-ended TW fault location, the relay uses the following expression to calculate the distance to the fault [2]:

$$d = \frac{(t_2 - t_1)}{2} v \qquad (13)$$

Where d is the calculated distance to the fault, and v is the speed of the traveling wave, which depends upon the L and C

intrinsic parameters per meter of the transmission line, but it is normally approximately by the speed of light [1].

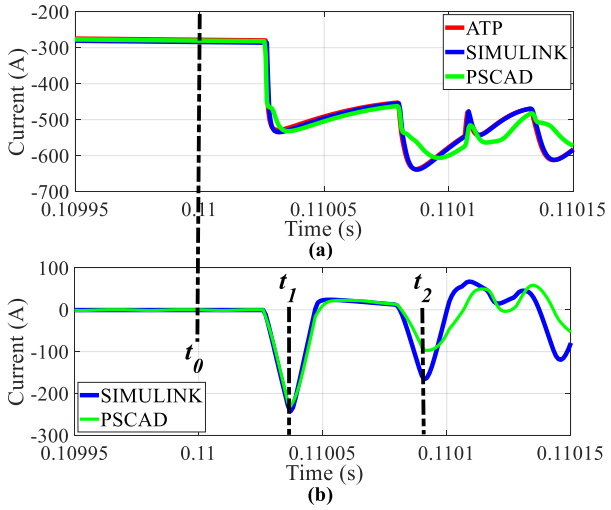

Figure 5. Traces out of simulation case 1. (a) Magnified segment of faulted current trace after fault inception. (b) TWs extracted by the relay, with the relay calculating a fault distance of 8.06 km.

From Figure 5-(a), notice that the current traces generated with the Simulink CHIL setup and the ATP offline simulation overlap on each other. However, the PSCAD current trace presents slight transient differences in the form of smoother transitions. Due to the overlap between the CHIL Simulink traces and the ATP traces, their extracted TWs will be the same. Thus, for the sake of better clarity in the TW comparisons, Figure 5-(b) only shows the extracted TWs from the Simulink and PSCAD simulations, which are the ones with more significant differences in transient dynamics. Even though both TWs traces in Figure 5-(b) have slightly different shapes in their amplitudes, both traces exhibit the same arrival times, with $t_1 = 0.1100906$ s and $t_2 = 0.1100363$ s. Using these arrival times in (13) gives an estimated fault distance of d = 8.06 km, which is the correct distance as depicted in Figure 4. This was an expected result, since both: the PI model of TL 2, and the load L_2 present an impedance discontinuity at Bus B_5 for the TW to be reflected properly, as formulated by (9). For this simulation case, the value of the reflection coefficient given by (11) provides a clear TW reflection for the relay to identify the correct fault location.

B. Simulation Case 2

This simulation case is almost the same as case 1, except for the transmission line model of TL 2, which is now a frequency-dependent model with the same intrinsic electrical parameters as the ones of TL 3. The same result in terms of fault location was expected due to load L_2 presenting an impedance discontinuity at Bus B_5, but results depicted in Figure 6 proved this hypothesis wrong. Notice again from Figure 6-(a) that the current traces right after fault inception maintained similar dynamics with some slight variations from the PSCAD trace. For this reason, the extracted TWs shown in Figure 6-(b) have similar dynamics. However, it is important to point out that while the first TW arrival ($t_1 = 0.1100365$ s) coincides with the one from simulation case 1, the second TW arrival time ($t_2 = 0.110123$ s) does not correspond with the fault distance. In fact, the calculated fault distance using (13), gives d = 12.8 km, which corresponds to the distance displayed on the relay's screen. The black arrow in Figure 6-(a) points out a barely noticeable bulge in the current trace that corresponds to the reflection that gives the correct fault distance. Nevertheless, such bulge is negligible for the relay's TW extraction algorithm.

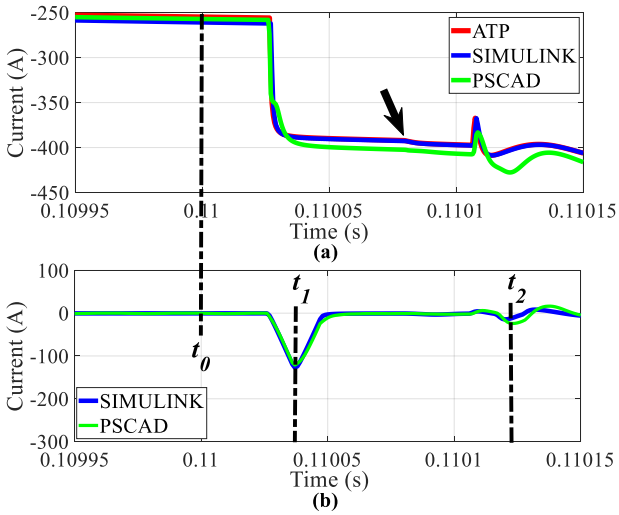

Figure 6. Traces out of simulation case 2. (a) Magnified segment of faulted current trace after fault inception. (b) TWs extracted by the relay, with the relay calculating a fault distance of 12.8 km.

This quite unnoticeable TW reflection is a consequence of twofold circumstances: i) the frequency-dependent model of TL 2 does not present a significant impedance discontinuity since now it is modeled using the same intrinsic parameters as TL 3. For this reason, the reflection coefficient given by (11) is almost zero; or the refraction coefficient given by (12) is close to unity. And ii) the load L_2 is not large enough to present a significant impedance discontinuity at bus B5. Therefore, most of the arriving TW's energy goes through TL 2, and the reflected energy is very low as pointed by the black arrow in Figure 6-(a).

A simulation case like this would require a more sensitive approach in terms of signal processing to capture low-energy TW events. The work reported in [6]–[8] seems to fit properly for these signal processing requirements.

The next two simulation cases will show the impact that L_2 could have in the TW reflections if this load type is changed in terms of rating (larger load) and type (capacitive load).

C. Simulation Case 3

This case is based upon simulation case 2, but this time the load L_2 was drastically increased from 2 MW to 150 MW to verify if this change has a significant impact on the TW reflections.

Once again, the CHIL Simulink current waveform overlaps the ATP simulation, as depicted in Figure 7-(a), with the

PSCAD trace showing small transient differences. Notice also that the extracted TWs depicted in Figure 7-(b) show not only a noticeable shape, but also their arrival times are on par with the correct fault distance. For this case, the exact TWs arrival times are: t_1 = 0.110037 s and t_2 = 0.110092 s. Based upon those times and using (13), gives d = 8.16 km, which is the exact distance displayed on the relay's screen.

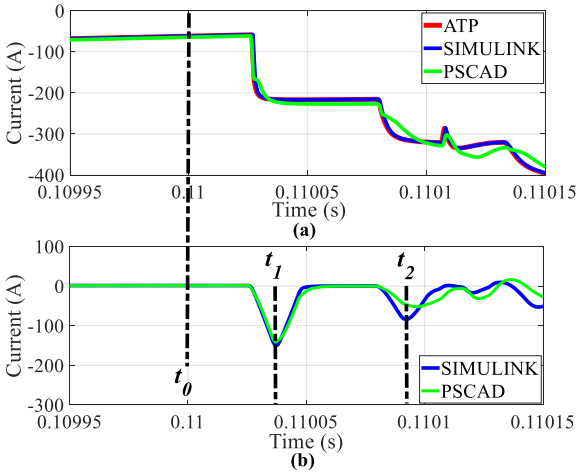

Figure 7. Traces out of simulation case 3. (a) Magnified segment of faulted current trace after fault inception. (b) TWs extracted by the relay, with the relay calculating a fault distance of 8.16 km.

D. Simulation Case 4

Finally, case 4 uses the same parameters as in simulation case 3, but replacing L_2 with a capacitor bank of 10 μF. No further in-depth qualitative analysis for this case will be made since the arrival times of the TWs correspond to the correct fault distance, as depicted in Figure 8. With t_1 = 0.110036 s and t_2 = 0.110092 s, using (13) with the aforementioned arrival times, gives d = 8.3 km.

Simulation cases 3 and 4 show that the load type and rating have a significant impact on the reflection and refraction coefficients when TL 2 is modeled as a frequency-dependent transmission line.

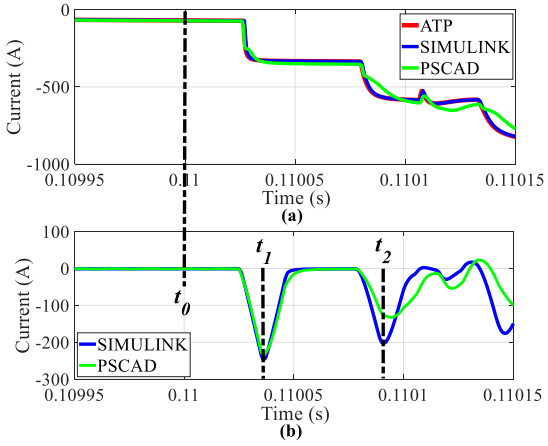

Figure 8. Traces out of simulation case 4. (a) Magnified segment of faulted current trace after fault inception. (b) TWs extracted by the relay, with the relay calculating a fault distance of 8.3 km.

V. CONCLUSIONS

With the aid of simulation cases performed in both: real-time, and offline scenarios; this paper points out the effects that different circuit elements can have over the TWs reflection and refractions coefficients. Base upon the generated TWs from each simulation, the corresponding qualitative analyses showed that under certain operation scenarios and simulation assumptions, the second arrival of TWs could not be detected by the relay under a single-ended scheme, and thus based upon delayed refections, the relay calculates the wrong fault distance. This type of analysis could set the basis when attempting to use TW relays to protect systems with more than one transmission lines connected in series.

ACKNOWLEDGMENT

Sandia National Laboratories is a multi-mission laboratory managed and operated by National Technology and Engineering Solutions of Sandia, LLC. a wholly owned subsidiary of Honeywell International, Inc., for the U.S Department of Energy's National Nuclear Security Administration under contract DE-NA-0003525.

REFERENCES

[1] E. O. Schweitzer III, B. Kasztenny, A. Guzman, V. Mynam, and H. J. Altuve Ferrer, *Locating Faults and Protecting Lines at the Speed of Light. Time Domain Principles Applied*, 1 Edition. SEL, 2018.

[2] E. O. Schweitzer, A. Guzman, M. V. Mynam, V. Skendzic, B. Kasztenny, and S. Marx, "Locating faults by the traveling waves they launch," in *2014 67th Annual Conference for Protective Relay Engineers, CPRE 2014*, 2014, pp. 95–110.

[3] A. Guzmán, V. V. Mynam, Mangapathirao Skendzic, and J. L. Eternod, "Directional Elements – How Fast Can They Be?," *44th Annu. West. Prot. Relay Conf.*, 2017.

[4] F. Wilches-Bernal *et al.*, "A Survey of Traveling Wave Protection Schemes in Electric Power Systems," *IEEE Access*, vol. 9. Institute of Electrical and Electronics Engineers Inc., pp. 72949–72969, 2021.

[5] M. Jimenez Aparicio, S. Grijalva, and M. J. Reno, "Fast Fault Location Method for a Distribution System with High Penetration of PV," in *54th Hawaii International Conference on System Sciences*, 2021.

[6] M. Jiménez Aparicio, M. J. Reno, P. Barba, and A. Bidram, "Multi-Resolution Analysis Algortihm for Fast Fault Classification and Location in Distribution Systems," *9th Int. Conf. Smart Energy Grid Eng.*, 2021.

[7] F. Wilches-Bernal, M. Jiménez Aparicio, and M. J. Reno, "An Algorithm for Fast Fault Location and Classification Based on Mathematical Morphology and Machine Learning," *2022 IEEE Innov. Smart Grid Technol. North Am. (ISGT NA)*, pp. 1–5, 2021.

[8] F. Wilches-Bernal, M. J. Reno, and J. Hernandez-Alvidrez, "A Dynamic Mode Decomposition Scheme to Analyze Power Quality Events," *IEEE Access*, vol. 9, pp. 70775–70788, 2021.

[9] M. Jimenez Aparicio and M. J. Reno, "Distribution System Modeling for Traveling Wave - based Zone Protection," *Electr. Power Syst. Res.*, 2021.

[10] A. Greenwood, *Electrical Transients in Power Systems*, 2 Edition. Wiley and Sons, 1991.

[11] N. Watson and Arrillaga Jos, *Power Systems Electromagnetic Transients Simulation*, 2 Edition. IET, 2018.

[12] R. Iracheta-Cortez, N. Flores-Guzman, and R. Hasimoto-Beltran, "Implementation of the frequency dependent line model in a real-time power system simulator," *Ing. e Investig.*, vol. 37, no. 3, pp. 61–71, Dec. 2017.

[13] Opal RT, "OPAL-RT News, Innovation & Breakthroughs," 2019.

[14] R. D. Kirby and G. Smelich, "No No Test Set? No Problem—Event Playback Simplifies Testing of Ultra-High-Speed Relays." [Online].